MJIT 2024 Malaysian Journal of Industrial Technology

ENERGY INVESTIGATION OF ADVANCED HYDROGEN AND POWER GENERATION SYSTEM BASED ON HYBRID SULFUR AND LITHIUM BROMIDE ABSORPTION POWER CYCLE

Salem A Yosaf.
Higher Institute of Science and Technology Al-Jufrah, Soknah, Libya
Email: salemyosaf1@gmail.com

Hamoda Gnaifaid.
Higher Institute of Science and Technolgy AL-Jufrah, Soknah, Libya
Email: gnaifaid@gmail.com

Farhat Eljelane.
Higher Institute of Science and Technology Al-Jufrah, Soknah, Libya.
Email: fjabubaker@gmail.com

*Corresponding author's email: salemyosaf1@gmail.com

ARTICLE INFO

Handling Editor: Rahimah Mahat

Article History:
Received 25 December 2023
Received in revised form 11 January 2024
Accepted 3 February 2024
Available online 15 March 2024

Keywords:
LBr-water absorption power cycle; Hybrid sulfur cycle; Power & hydrogen production; The first law of thermodynamics.

ABSTRACT

The study aims to improve the solar hybrid sulfur cycle (Shysc) thermal efficiency. The Shysc waste heat is utilized for power generation by integrating the lithium bromide-water absorption power cycle (LiBr-H_2O APC). The developed cogeneration integrated system produces 4.967 moles of hydrogen and 1.22 MW at an efficiency of 60% according to the first law of thermodynamics. The advanced system is 30% more efficient than a conventional hybrid sulfur cycle (Chysc). The efficiency development is due to utilizing the waste heat in the Chysc and converting it into useful power by (LiBr-H_2O APC). Increasing the process's consumed energy harms the system's efficiency. The largest amount of energy is consumed by the thermal cracking process, which reached 69% of the overall energy. Likewise, the electrolyser performance affects the overall efficiency. As the electrolyser performance increases, the amount of converted sulfur dioxide increases and thus, leads to an increase in the amount of produced hydrogen, which enhances the system's efficiency.

1.0 Introduction

Hydrogen, widely acknowledged as a pristine energy carrier of paramount significance, stands as a vanguard among pivotal energy sources [1]. Its combustion yields a noteworthy thermal energy output, measuring 120 MW/kg when considered in the context of its lower heating value. Notably, the chemical interaction between molecular hydrogen (H_2) and oxygen (O_2) exhibits an absence of deleterious emissions, leading exclusively to the formation of water and the liberation of energy. This commendable attribute renders hydrogen a distinguished exemplar of an environmentally conscientious fuel source.

It is imperative to underscore that hydrogen, while not indigenous to the natural environment in an unadulterated form, is prevalently encountered in nature as a constituent of water, wherein it is chemically combined with oxygen. The manifold advantages intrinsic to hydrogen as an energy vector have propelled extensive scholarly inquiry, centering on its synthesis and its potential role as a sustainable alternative to conventional fossil fuels.

The domain of hydrogen production encompasses a spectrum of methodologies, among which the electrochemical process of water electrolysis and the electrochemical reaction involving liquid sulfur dioxide and water within an electrolytic apparatus, commonly referred to as Hysc, is notably prominent [2,3].

In the primary stage of the Hysc process, a solution of sulfuric acid is subjected to thermal treatment, leading to the conversion of sulfuric acid into sulfur trioxide (SO3) and water. Subsequently, the temperature of the resultant products is elevated, facilitating the transformation of sulfur trioxide gas into oxygen and sulfur dioxide (SO2), as expounded by the chemical equations denominated in Eq. 1 and Eq. 2. The aqueous solution containing sulfur dioxide is then channelled to the electrolytic cell, where it engages in a transformative interaction with water, ultimately yielding hydrogen, as articulated by Eq. 3. The penultimate phase within this cyclic process involves the concentration of the acid solution, a crucial endeavor in the aftermath of the electrochemical analysis process [4, 5].

$$H_2SO_4 = SO_3 + H_2O \quad (1)$$

$$SO_3 = SO2 + 0.5O2 \quad (2)$$

$$SO2 + 2H_2O = H_2SO_4 + 2H^+ + 2e^- \quad (3)$$

Numerous scholarly investigations have made substantial contributions to the progressive evolution of the (HyS). Recent inquiries have advanced our understanding, affirming that the thermal efficiency of the HyS cycle can now attain remarkable levels, within the range of 30-35% [6, 7]. It is imperative to emphasize that the production process of the HyS cycle necessitates a high-temperature energy source, typically surpassing 1000 Kelvin, thereby prompting the utilization of nuclear energy as a prominent energy source [8, 9]. However, in a notable contemporary development, the evolution of solar collector technology has reached a juncture where these collectors can provide thermal energy surpassing 1000 Kelvin. Consequently, solar energy has emerged as a viable alternative for powering the HyS cycle [10-12]. Notably, in the context of solar hydrogen production, recent studies have demonstrated the feasibility of converting solar energy into hydrogen at a commendable conversion efficiency of approximately 10% [7, 13].

The (LiBr-H2O APC) is a pivotal technological solution employed for the conversion of low-temperature thermal energy into electrical power, as documented by relevant literature [14]. This specialized cycle, which has been systematically developed, extends its utility beyond

power generation to encompass the efficient extraction of cold energy. It accomplishes this dual objective by harnessing a variety of low-temperature energy sources, including but not limited to geothermal energy, various renewable energy sources, and waste heat [15, 16].

The distinguished work of Alperen et al. has significantly contributed to the maturation of the LiBr-H2O APC. Their innovation centers on the incorporation of a water condenser, a development that serves to enhance the volume of water vapor entering the turbine. This augmentation, in turn, leads to a substantial increase in power production [17]. Additionally, the cycle has witnessed further refinements through the integration of a two-phase ejector at the absorber inlet. This enhancement plays a pivotal role in lowering the absorber's pressure, thereby affecting an overall enhancement of cycle efficiency[18].

Notably, prior research has harnessed the electrical energy generated by the LiBr-H2O APC to operate an electrolyzed for hydrogen production. Following our previous study, the investigation delineates the possibility of generating 1.15 kilograms of hydrogen, thereby demonstrating varying efficiencies of 6% and 18%. These efficiencies have been rigorously assessed in conformity with the foundational tenets of the first and second laws of thermodynamics. The cost associated with this hydrogen production does not exceed 2.43 US dollars per kilogram, as elucidated in our research findings [19].

In recent developments, solar collectors have undergone significant enhancements, incorporating the innovative use of sand as a thermal energy storage medium. These advancements have propelled the operational temperature of solar collectors to levels exceeding 1000 Kelvin, as substantiated by pertinent scholarly studies [20, 21]. This noteworthy achievement has laid the foundation for effectively harnessing solar energy to fulfil high-temperature energy demands, including applications within the context of the hybrid sulfur cycle [7, 22]. These advancements augur the potential for solar energy to emerge as a compelling alternative to conventional fossil fuels in high-temperature industrial processes.

Drawing upon the technological progress, the present study has leveraged the waste heat energy generated by the cycle, underscoring the feasibility of integrating the Absorption Power Cycle (APC) for the simultaneous production of hydrogen and electrical power. This integrated approach signifies a significant stride toward harnessing renewable energy sources, optimizing energy utilization, and promoting sustainable energy conversion technologies.

2.0 Process Flow Sheet Diagram

The developed hybrid sulfur cycle is summarized in five main processes: Solution concentration, thermal cracking, oxygen separation, electrochemical reaction, and power generation process, which is demonstrated in Figure 1.

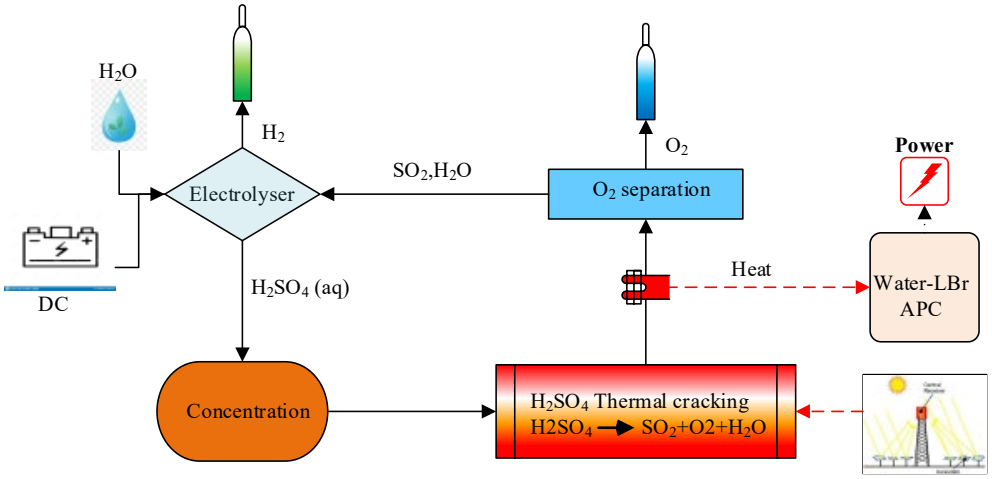

Figure 1. Schematic diagram of advanced (Hysc)-(LiBr-H_2O APC) system

In more detail, Attachment 1&2 presents the finer details of the advanced (Hysc)-(LiBr-H_2O APC). The energy and hydrogen production processes in the advanced system begin with the thermally concentrating of solution (1-2). The temperature of the concentrated sulfuric acid solution is raised in the superheater to evaporate, and thus the acid decomposes into SO_2 and water (4-6). The temperature of the steam in the decomposer is raised to a temperature (1520K) at which most of the SO_3 converts to SO_2 and O_2 (6-7). The thermal energy of the steam is recovered through a series of 3 heat exchangers (7-10). The temperature of the steam drops, causing a little condensation, and converting the remaining sulfur SO_3 to acid (10). SO_2 is separated, and the liquid, consisting mostly of an acid solution, is sent to the mixing tank (10B). The gas, which consists mostly of (SO_2) is cooled to turn into a mixture phase before raising the pressure to the absorber pressure (12A). The gas pressure is raised to the absorber pressure (12 bar) in two stages (11-12) and then (13-15). The heat generated as a result of gas pressurized is recovered (16) and (13). The liquid gas pressure is lifted directly to the absorber pressure (12B-17). At the absorber inlet, the mixture is cooled to 313K and the O_2 is then separated and collected as an additional cycle product (17-O_2). The liquid is heated downstream of the absorber through the heat exchanger (18-20). The mixture enters distillation device 1, and excess water is separated and recycled to the absorber (21A-21B).

SO_2 enters the electrolyser at the liquid phase and reacts with water to produce hydrogen. In addition to hydrogen, the reaction produces sulfuric acid and heat, which contributes to raising the temperature to 370 K. Because of this, the analyser does not need external heat.

The study assumes that 40% of the SO_2 reacts to produce hydrogen. The mixture coming out of the electrolyser containing the residual (SO2) is heated before being fed into the distiller 2 (25-26). The distillate residual gas is sent back to the electrolyser (29-23). As for the acidic solution, it is sent to the tank after recovering part of its energy (27-28), thus completing the hybrid cycle.

The (LiBr-H_2O) cycle is operated by heat recovered from the hybrid cycle. Two absorption cycles are integrated to utilize the recovered energy as much as possible. The (LiBr-H_2O) cycle begins by raising the temperature of the weak lithium bromide solution in the heat exchangers so that part of it is evaporated (30) and (39A&B). Water vapor is separated and enters the turbine to generate power (31) and (40). The energy of the concentrated solution is recovered by the heat exchangers, and the mixture is then cooled in the absorber where the absorption process takes place (32-35) and (42-48). The saturated solution pressure and temperature are

raised by the pump and heat exchangers respectively, thus completing the cycle (37-30) and (49-39A&B).

DWSIM was utilized to simulate the process and generate material and mass, energy balance. DWSIM is an open-source, chemical process simulator compliant with computer-aided process engineering (CAPE) [23].

3.0 Result and Discussion

The advanced system consumes 4031.45 kW of energy to produce 4.96 moles of hydrogen and 1.22W. Each stage of the system consumes a portion of energy, directly affecting the system's efficiency. To determine the effect of each stage on the overall efficiency, the amount of consumed energy in each stage is calculated, and its impact on the overall efficiency is studied.

3.1 Process Energy Demand

The energy consumed by each process and the parameters affecting it are calculated and studied. As well as studying its impact on the overall system's efficiency.

3.1.1 Solution Concentration Process

Hydrogen production processes in the hybrid cycle begin with the concentration process. The required acid concentration for the process is 62%, which requires heating the solution to 380,504 K, consuming an energy of 4.73 kJ/mol H_2, which represents 0.582% of the total energy.

3.1.2 Sulfuric Acid Thermal Cracking

The main purpose of the process is SO_2 production. The process occurs at 1520K and consumes a thermal energy of 565.86 kJ / mol hydrogen, which is 69.613% of the overall energy. Fig.2 demonstrates the effect of decomposer temperature on the SO_3 conversion rate. As the figure shows, the rate increases with increasing the decomposer temperature. At 1573 most of the SO_3 gas converts into SO_2.

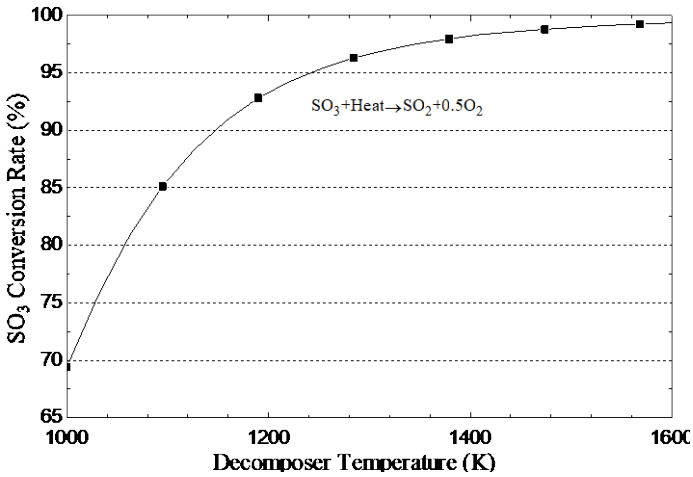

Figure 2. SO_3 conversion rate

3.1.3 Gas comproession process

The pressure of the thermal cracking products is lifting to the absorption pressure of 12 bar. Pressure lifting equipment consumes an energy of 18.59 kJ/mole, which constitutes 2.287% of the total energy.

3.1.4 Oxegyen Separation Process

O_2 is separated through two stages. The beginning stage is absorbing SO_2 by water (SO_2 aqueous). O_2 remains only at the gas phase to be separated and collected. Figure 3 demonstrates the effect of the O_2 mass fraction on the absorbed SO_2. As the O_2 mass increases in the mixture, the amount of absorbed SO_2 decreases. As for the water fraction in the mixture, it has a positive effect on the absorption process. In contrast to the first stage (absorption), the SO_2 distillation consumes thermal energy of 61.65 kJ/mol $_{(H2)}$ which equals 7.59% of the system's energy. Figures 4a and b show the effect of the amount and temperature of the water on the consumed energy, as well as on the distillation temperature. The distillation energy (column 1) decreases with the increase in the inlet water temperature, while the distillation temperature is almost steady. Figure 4b demonstrates that distillation energy increases with increasing water mass fraction. The more water there is, the more heat is needed to heat it and separate the SO_2. Because of this, the excess water should be avoided. In addition, Figure 4b, plots the effect of O_2-SO_2 mass fraction on the distillation energy, the ratio does not greatly affect the energy.

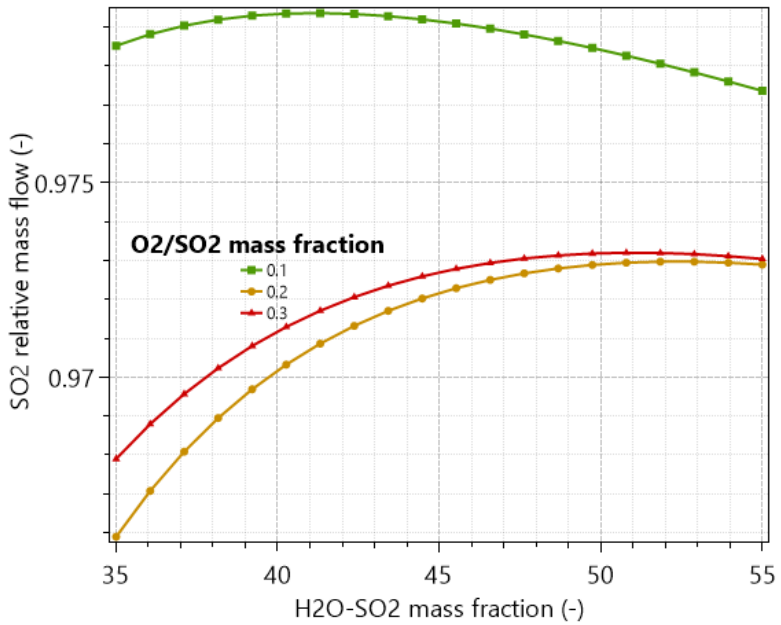

Figure 3. The effect of oxygen and water on the SO2 solubility

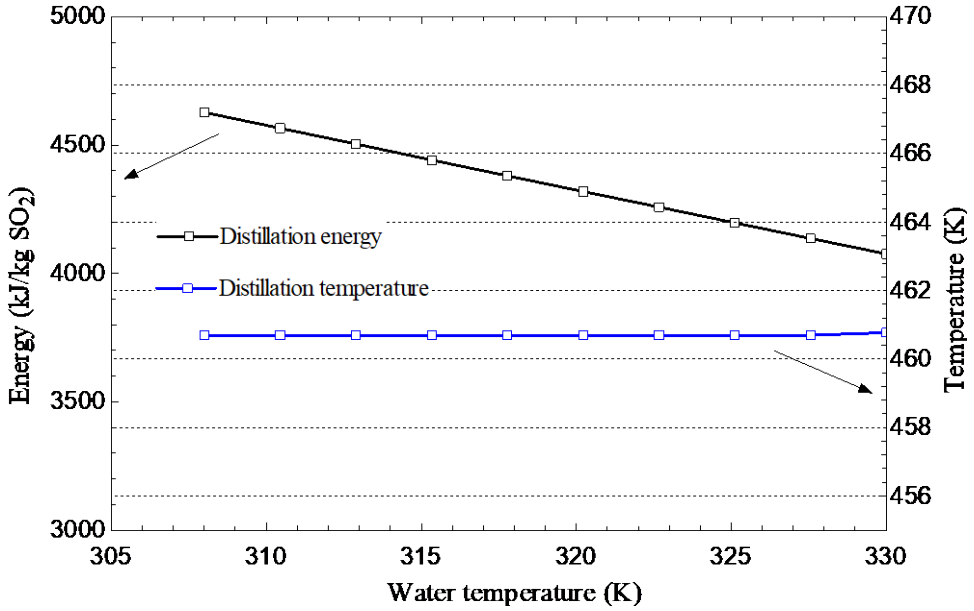

Fig. 4 (a)

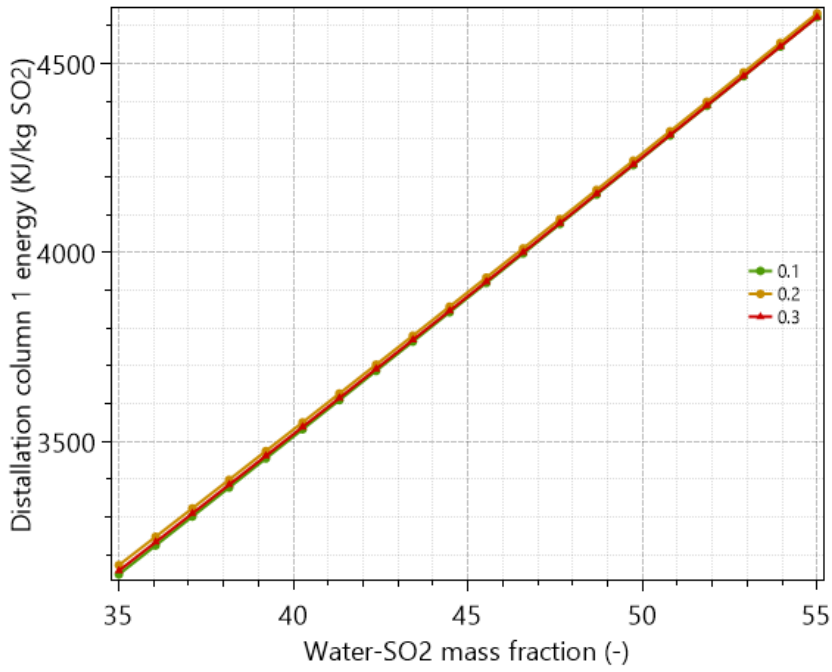

Fig. 4 (b)

Figure 4. Effect of the water temperature (a) and water fraction (b) on the distillation column1 energy.

3.1.5 Electrochemical Hydrogen Generation

4.96 moles of hydrogen are produced using a reversible and operating voltage of 0.158, and 0.6 volts respectively, with an electric power of 115 kJ/mol$_{(H2)}$ and a current density of 500

mA/cm^2. 40% of SO_2 reacts with water to produce this amount, consuming 14.148% of the system's total energy.

3.1.6 Distillation of Excess SO_2

The final stage to complete the system cycle is the distillation of SO_2 leaving the electrolyser that has not reacted with water (distillation column 2). It is extracted in distiller 2, consuming an energy of 47 kJ/mol, which constitutes 5.786% of the total energy. The electrolyser performance affects the amount of remaining SO_2, which in turn affects the amount of energy needed for the distillation. Figure 5 shows that the consumed energy in the distillation device depends on the electrolyser efficiency. By increasing the electrolyser performance, the amount of remaining gas decreases and thus leads to a reduction in the energy. As for the temperature distiller, it is not affected by the electrolyser performance.

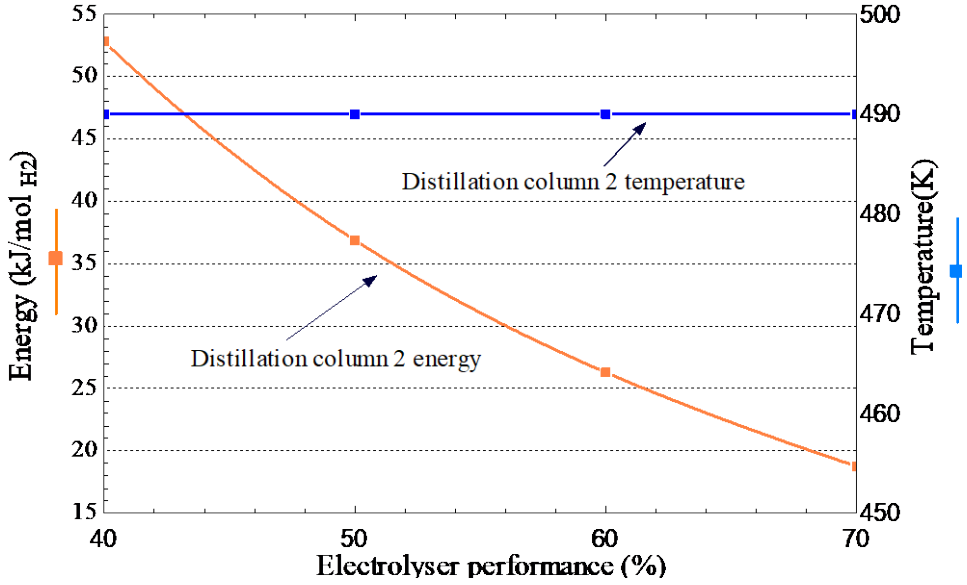

Figure 5. Effect of electrolyser performance on the distillation column2 energy.

Figure 6 studies the effect of water mass fraction on distillater2 energy and distillation temperature. Increasing the water mass fraction increases the distillation energy because the energy is consumed for heating and evaporating the excess water. While the distillation temperature decreases, due to the increase in the proportion of solvent.

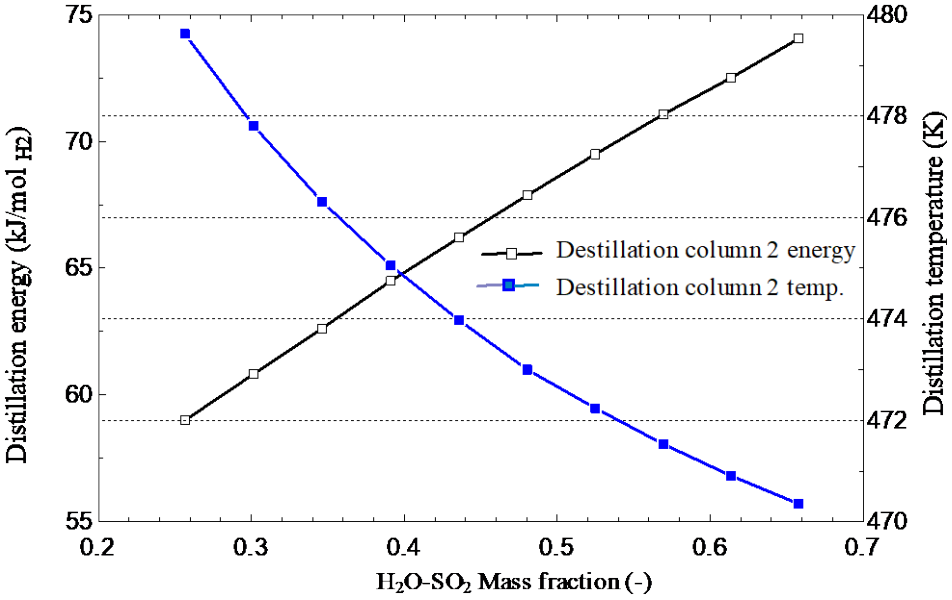

Figure 6. Effect of water fraction on distillation column2 energy.

4.0 System Energy Efficiency

The efficiency of any thermodynamic system is the percentage of the gained energy to the expended energy. The process energy efficiency of a conventional hybrid cycle which only produces hydrogen is 30% based on the hydrogen low value, which is consistent with most previous studies. By integrating the absorption power cycle and utilizing the heat recovery, an additional 0.246 MJ/mol($_{H2}$) is produced, causing an increase in the total efficiency of the system to approximately 60%.

The system efficiency is affected by the decomposer temperature. Figure 7 shows the efficiency curve of the conventional hybrid cycle, as well as the curve of the advanced system. The optimum value of efficiency is achieved at 1520 K.

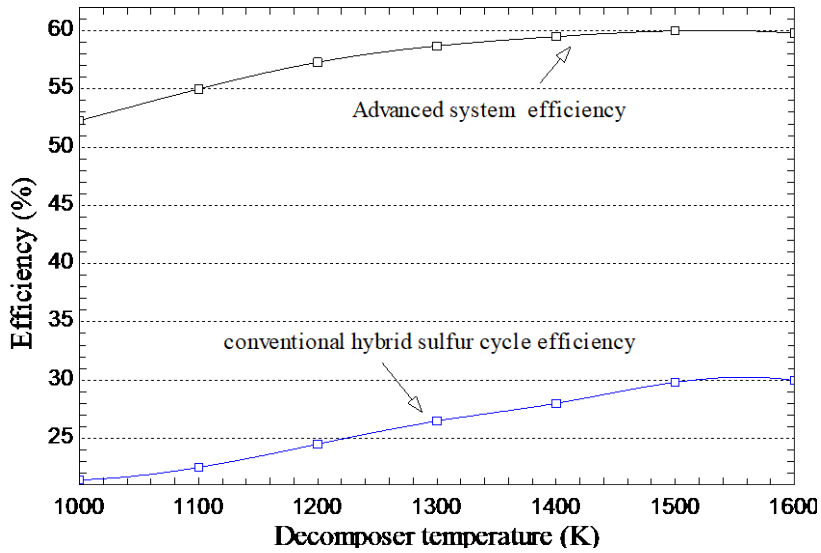

Figure 7. Effect of the decomposer temperature on the system efficiency.

5.0 Conclusions and Outlook

1. The system under examination has demonstrated the production of 1.22 MW of power and the generation of 4.97 moles/s of hydrogen. This power production was achieved with a total energy consumption of 4031.45 kW, resulting in a commendable thermal efficiency of 60%.
2. It is noteworthy that a substantial portion of the total energy consumption, specifically 69%, is consumed by the thermal cracking process. This insight underscores the significance of addressing the energy demands associated with this particular step
3. Further investigation reveals that an increase in the oxygen mass fraction within the absorber has the effect of reducing the rate at which gas is dissolved in the water. Consequently, a higher energy input is required to achieve the desired results.
4. Conversely, the presence of excess water within the absorber also imposes a greater energy demand, emphasizing the importance of minimizing excess water.
5. Notably, improvements in electrolyser performance yield a dual benefit: a reduction in energy consumption and an increase in hydrogen production. This, in turn, contributes to an overall enhancement in the system's efficiency.

In light of these findings, there is potential for future studies to explore the integration and evaluation of the Hybrid Sulphur Cycle (HyS) with a power cycle that exhibits superior thermal efficiency in comparison to the water-LiBr absorption cycle. Additionally, the system's efficiency can be further augmented by capitalizing on waste heat for various auxiliary purposes, including water desalination and heating. These avenues for improvement hold promise in the pursuit of more efficient and sustainable energy systems.

6.0 References

[1] G. F. Naterer, I. Dincer, and C. Zamfirescu, *Hydrogen production from nuclear energy*. Springer, 2013.

[2] P. Nikolaidis and A. Poullikkas, "A comparative overview of hydrogen production processes," *Renewable and sustainable energy reviews,* vol. 67, pp. 597-611, 2017.

[3] K. Christopher and R. Dimitrios, "A review on exergy comparison of hydrogen production methods from renewable energy sources," *Energy & Environmental Science,* vol. 5, no. 5, pp. 6640-6651, 2012.

[4] M. Gorensek, W. Summers, C. Boltrunis, E. Lahoda, D. Allen, and R. Greyvenstein, "Hybrid sulfur process reference design and cost analysis," Savannah River Site (SRS), Aiken, SC (United States)2009.

[5] M. B. Gorensek and W. A. Summers, "Hybrid sulfur flowsheets using PEM electrolysis and a bayonet decomposition reactor," *International Journal of Hydrogen Energy,* vol. 34, no. 9, pp. 4097-4114, 2009.

[6] A. G. Niehoff *et al.*, "Process modelling and heat management of the solar hybrid sulfur cycle," *International Journal of Hydrogen Energy,* vol. 40, no. 13, pp. 4461-4473, 2015.

[7] M. B. Gorensek, C. Corgnale, and W. A. Summers, "Development of the hybrid sulfur cycle for use with concentrated solar heat. I. Conceptual design," *International Journal of Hydrogen Energy,* vol. 42, no. 33, pp. 20939-20954, 2017.

[8] W. A. Summers, M. R. Buckner, and M. B. Gorensek, *The hybrid sulfur cycle for nuclear hydrogen production*. Citeseer, 2005.

[9] R. Pinsky, P. Sabharwall, J. Hartvigsen, and J. O'Brien, "Comparative review of hydrogen production technologies for nuclear hybrid energy systems," *Progress in Nuclear Energy,* vol. 123, p. 103317, 2020.
[10] S. U. Batgi and I. Dincer, "A solar driven hybrid sulfur cycle based integrated hydrogen production system for useful outputs," *International Journal of Hydrogen Energy,* 2023.
[11] R. Liberatore, M. Ferrara, M. Lanchi, and L. Turchetti, "Integration of photovoltaic and concentrated solar thermal technologies for H2 production by the hybrid sulfur cycle," in *AIP Conference Proceedings*, 2017, vol. 1850, no. 1: AIP Publishing.
[12] B. Coelho, A. Oliveira, and A. Mendes, "Concentrated solar power for renewable electricity and hydrogen production from water—a review," *Energy & Environmental Science,* vol. 3, no. 10, pp. 1398-1405, 2010.
[13] S. Yosaf, H. Gniaifaid, and A. Abrahem, "Thermodynamic evaluation of hybrid sulfur cycle based on integration system for hydrogen production."
[14] V. Novotny, J. Spale, J. Pavlicko, D. J. Szucs, and M. Kolovratnik, "Experimental development of a lithium bromide absorption power cycle," *Renewable Energy,* vol. 207, pp. 321-347, 2023.
[15] V. Novotny, V. Vodicka, J. Mascuch, and M. Kolovratnik, "Possibilities of water-lithium bromide absorption power cycles for low temperature, low power and combined power and cooling systems," *Energy Procedia,* vol. 129, pp. 818-825, 2017.
[16] B. H. Gebreslassie, E. A. Groll, and S. V. Garimella, "Multi-objective optimization of sustainable single-effect water/Lithium Bromide absorption cycle," *Renewable energy,* vol. 46, pp. 100-110, 2012.
[17] A. Tozlu, S. A. Yosaf, and H. Özcan, "Thermodynamic feasibility analysis of a newly modified absorption power cycle running with LiBr-water," *Environmental Progress & Sustainable Energy,* vol. 40, no. 1, p. e13483, 2021.
[18] H. Ozcan and S. Yosaf, "Energy and exergy analysis of advanced absorption power cycles using salt-water mixtures as working fluids," *International Journal of Exergy,* vol. 25, no. 3, pp. 187-202, 2018.
[19] S. Yosaf and H. Ozcan, "Exergoeconomic investigation of flue gas driven ejector absorption power system integrated with PEM electrolyser for hydrogen generation," *Energy,* vol. 163, pp. 88-99, 2018.
[20] O. A. Radwan and J. D. Humphrey, "Uses of sands in solar thermal technologies," *Solar Energy Materials and Solar Cells,* vol. 261, p. 112533, 2023.
[21] M. Diago, A. C. Iniesta, A. Soum-Glaude, and N. Calvet, "Characterization of desert sand to be used as a high-temperature thermal energy storage medium in particle solar receiver technology," *Applied Energy,* vol. 216, pp. 402-413, 2018.
[22] C. Corgnale, Z. Ma, and S. Shimpalee, "Modeling of a direct solar receiver reactor for decomposition of sulfuric acid in thermochemical hydrogen production cycles," *International Journal of Hydrogen Energy,* vol. 44, no. 50, pp. 27237-27247, 2019.
[23] K. Tangsriwong, P. Lapchit, T. Kittijungjit, T. Klamrassamee, Y. Sukjai, and Y. Laoonual, "Modeling of chemical processes using commercial and open-source software: A comparison between Aspen Plus and DWSIM," in *IOP Conference Series: Earth and Environmental Science*, 2020, vol. 463, no. 1, p. 012057: IOP Publishing.

Attachment 1. Advanced System flow diagram

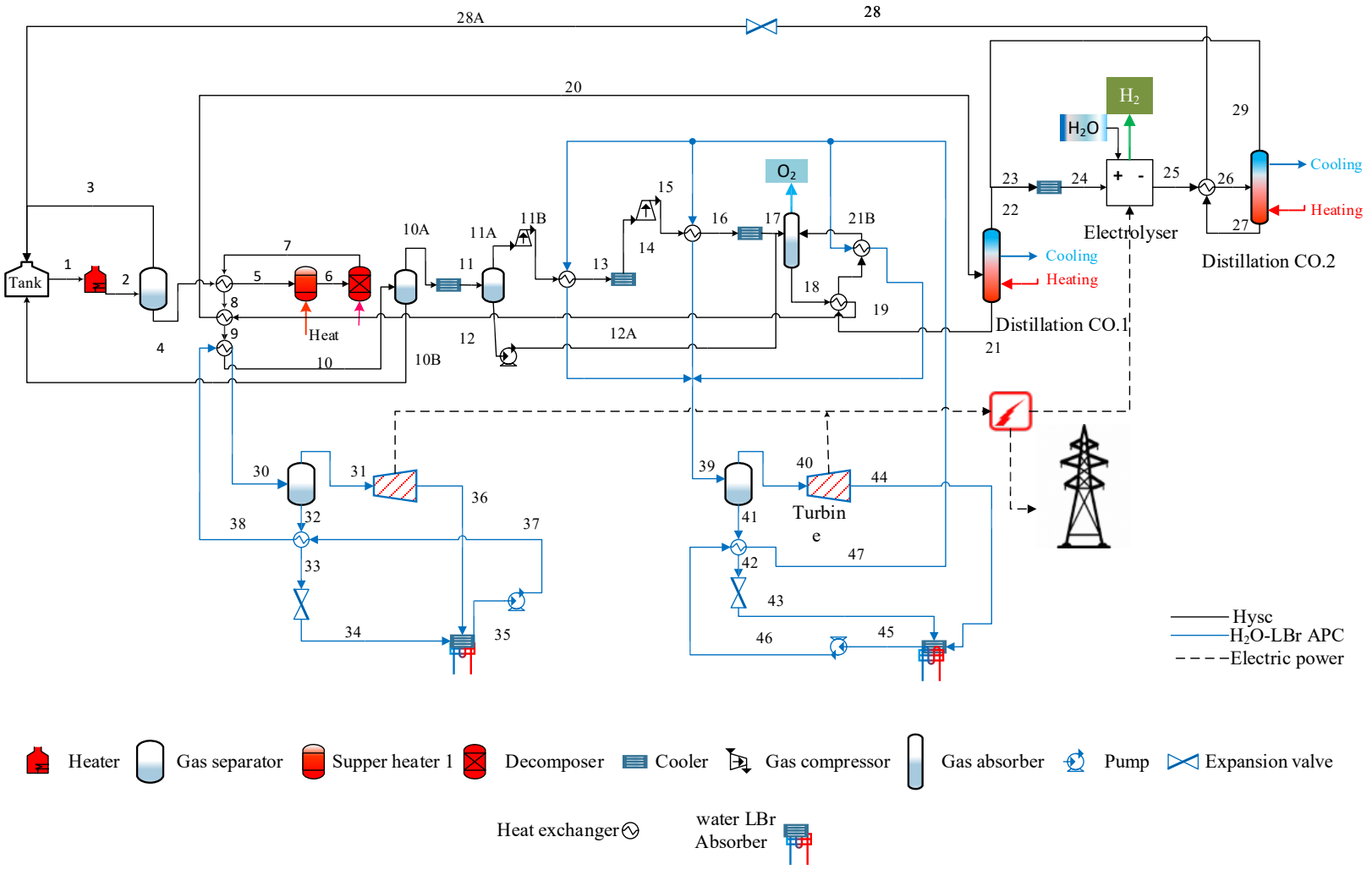

Attachment 2. Advanced system process streams statement

Stream (No)	Pressure (bar)	Temperature (K)	Mass fraction (-)						Vapure fraction
			H2O	H2SO4	SO3	SO2	O2	H2	
1	1	381.3	0.503	0.497	0	0	0	0	0.3
2	1	381.5	0.503	0.497	0	0	0	0	0.34
3	1	381.5	0.98	0.02	0	0	0	0	1
4	1	381.5	0.38	0.62	0	0	0	0	0
5	1	419	0.38	0.62	0	0	0	0	0.91
6	1	673	0.49	0	0.51	0	0	0	1
7	1	1520	0.49	0	0.005	0.4	0.1	0	1
8	1	702	0.49	0	0.005	0.4	0.1	0	1
9	1	457	0.49	0	0.005	0.4	0.1	0	1
10	1	352	0.49	0.006	0	0.4	0.1	0	1
10A	1	352	0.199	0	0	0.64	0.16	0	1
10B	1	352	0.984	0.016	0	0	0	0	0
11	1	313	0.199	0	0	0.64	0.16	0	0.616
11A	1	313	0.023	0	0	0.782	0.195	0	1
11B	4	460	0.023	0	0	0.782	0.195	0	1
12	1	313	0.999	0.001	0	0	0	0	0
12A	12	313.1	0.999	0.001	0	0	0	0	0
13	4	348	0.023	0	0	0.782	0.195	0	1
14	4	340	0.023	0	0	0.782	0.195	0	1
15	12	462	0.023	0	0	0.782	0.195	0	1
16	12	347.78	0.023	0	0	0.782	0.195	0	0.967
17	12	313	0.023	0	0	0.782	0.195	0	0.612
18	12	345	0.936	0	0	0.064	0	0	0
O_2	12	308	0	0	0	0	1	0	1
19	12	459.5	0.936	0	0	0.064	0	0	0.52
20	12	460	0.936	0	0	0.064	0	0	0.86
21	12	461.2	1	0	0	0	0	0	0.867
22	12	342.7	0.934	0	0	0.046	0	0	0.002
23	12	339	0.0278	0	0	0.9722	0	0	0
24	12	313	0.0278	0	0	0.9722	0	0	0
25	12	378	0.026	0.39	0	0.584	0	0	0.58
H2	12	378	0	0	0	0	0	1	1
26	12	446.88	0.026	0.39	0	0.584	0	0	0.653
27	12	502.7	0.01	0.99	0	0	0	0	0
28	12	380	0.01	0.99	0	0	0	0	0
28A	1	380	0.01	0.99	0	0	0	0	0
29	12	336	0.002	0	0	0.998	0	0	0.004

LiBr-H_2O APC 1 process streams statement

Stream (No)	Pressure (bar)	Temperature (K)	Mass fraction(-)		Vapour fraction (-)
			H2O	LiBr	
30	14.5	441	0.33	0.67	0.69
31	14.5	441	1	0	1
32	14.5	441	0.006	0.994	0
33	14.5	326	0.006	0.994	0
34	0.144	326	0.006	0.994	0
35	0.144	308	0.33	0.67	0
36	0.144	326	1	0	0.89
37	14.5	308.4	0.33	0.67	0
38	14.5	350	0.33	0.67	0

LBr-H_2O APC 2 process streams statement

Stream (No)	Pressure (bar)	Temperature (K)	Mass fraction (-)		Vapour fraction (-)
			H2O	LiBr	
39	18	447	0.33	0.67	0.69
40	18	447	1	0	1
41	18	447	0.006	0.994	0
42	18	341	0.006	0.994	0
43	0.144	341	0.006	0.994	0
44	0.144	326	1	0	0.81
45	0.144	308	0.33	0.67	0
46	18	308.47	0.33	0.67	0
47	18	346	0.33	0.67	0